A Density Functional Theory Study of the Magnetic Exchange Coupling in Dinuclear Manganese(II) Inverse Crown Structures

Ederley Vélez, Antonio Alberola,* and Víctor Polo*

Departament de Química Física i Analítica, Universitat Jaume I, 12071, Castelló, Spain, Departamento de Química Orgánica y Química Física, Universidad de Zaragoza, 50006, Zaragoza, Spain, and Instituto de Biocomputación y Física de los Sistemas Complejos, Edificio Cervantes, Corona de Aragón 42, Zaragoza 50009, Spain

Received: July 28, 2009; Revised Manuscript Received: October 12, 2009

The magnetic exchange coupling constants between two Mn(II) centers for a set of five inverse crown structures have been investigated by means of a methodology based on broken-symmetry unrestricted density functional theory. These novel and highly unstable compounds present superexchange interactions between two Mn centers, each one with $S = {}^5/_2$ through anionic "guests" such as oxygen, benzene, or hydrides or through the cationic ring formed by amide ligands and alkali metals (Na, Li). Magnetic exchange couplings calculated at B3LYP/6-31G(d,p) level yield strong antiferromagnetic couplings for compounds linked via an oxygen atom or hydride and very small antiferromagnetic couplings for those linked via a benzene molecule, deprotonated in either 1,4- or 1,3- positions. Analysis of the magnetic orbitals and spin polarization maps provide an understanding of the exchange mechanism between the Mn centers. The dependence of *J* with respect to 10 different density functional theory potentials employed and the basis set has been analyzed.

1. Introduction

From among the large quantity of manganese compounds synthesized and isolated to date a very special set of binuclear manganese compounds is the family known as inverse crown ether (ICE) ring structures.[1,2] These compounds can be described as an anionic core (X), which is surrounded by a cationic ring, made up of alternating nitrogen and metal atoms (M^1 and M^2) (see Scheme 1). Topologically they show a remarkable similarity with conventional crown ethers, although with interchanged Lewis acidic/basic positions. These complexes have received much attention lately since they can behave as oxygen scavengers[3] and provide synthetic chemists with the possibility of fine-tuning the reactivity profiles of lithium amides, used as selective deprotonating agents[4] in organic chemistry, by introducing a second metal center. Recently the family of ICEs has been extended to include transition metals in the cationic ring.[5−8] In these compounds the M^1 position is occupied by an alkaline metal, whereas the M^2 position corresponds to a Mn(II) ion. Other ICEs incorporating magnetic transition metals have been recently synthesized and characterized.[9] These novel structures are good candidates to study the magnetic exchange interactions between the Mn(II) centers, since they can be treated as well isolated dimers with no interactions with surrounding molecules and no other magnetic exchange pathway available.

These structures where anionic "guests" can connect two Mn(II) centers provide new ways of magnetic coupling to be explored. The Mn(II) sodium $[(hmds)_4Na_2Mn_2O]$ (**1**) (HMDS=1,1,1,3,3,3-hexamethyldisilazide) and lithium $[(tmp)_4Li_2Mn_2O]$ (**2**) (TMP = 2,2,6,6-tetramethylpiperidine) compounds containing an oxide (O^{2-}) core (see Scheme 2) were reported by Mulvey et al.,[6] and although they were crystallographically characterized, its high instability prevented their magnetic characterization. An extension of the cationic ring allows the accommodation of a doubly deprotonated benzene molecule in the anionic position in what are the first benzene-bridged dimanganese compounds for which a magnetic study has been reported. In these compounds the benzene molecule is deprotonated in either *p*-$[(tmp)_6Na_4(1,4\text{-}Mn_2C_6H_4)]$ (**3**), or *m*-$[(tmp)_6Na_4(3,5\text{-}Mn_2C_6H_3CH_3)]$ (**4**).[7] Finally, a new Mn(II) ICE has been recently synthesized and characterized[10] holding hydride in the anionic core $[Na_2Mn_2(\mu\text{-}H)_2\{N(iPr)_2\}_4]\cdot 2$ toluene (**5**) showing medium antiferromagnetic coupling between the Mn(II) centers.

The strength of the magnetic exchange interaction *J* depends on the superexchange communication pathway between the spins, which is in itself dependent upon both the geometry and nature of the bridging ligand. In this article we focus our attention on the theoretical study of a series of ICE complexes (**1**)−(**5**) in order to rationalize their possible exchange pathways and to complement the experimental magnetic measurements. Recently, theoretical studies on Mn dimers have been performed using ab initio methodologies on Mn_2 showing weak antiferromagnetic coupling.[11,12] However, expensive quantum-chemical methods such as CASSCF or CI approaches can be used only for model systems. The treatment of Mn dimer complexes embedded in larger molecular systems requires the use of broken symmetry density functional theory (BS-DFT) techniques using

SCHEME 1: General Structure of Inverse Crown Compounds

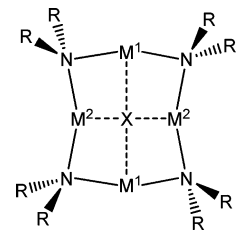

* To whom correspondence should be addressed. E-mail:. Antonio.alberola@qfa.uji.es (A.A.); vipolo@unizar.es (V.P.). Phone: (+34) 964-728071. Fax: (+34) 964-728066.

10.1021/jp907200u CCC: $40.75
Published on Web 10/28/2009

SCHEME 2: Mn(II) Dimers Studied in This Work: (1) R = −Si(CH$_3$)$_3$; (2) R = −TMP; (3) R = −TMP; (4) R = −TMP; (5) R = −N(iPr)$_2$

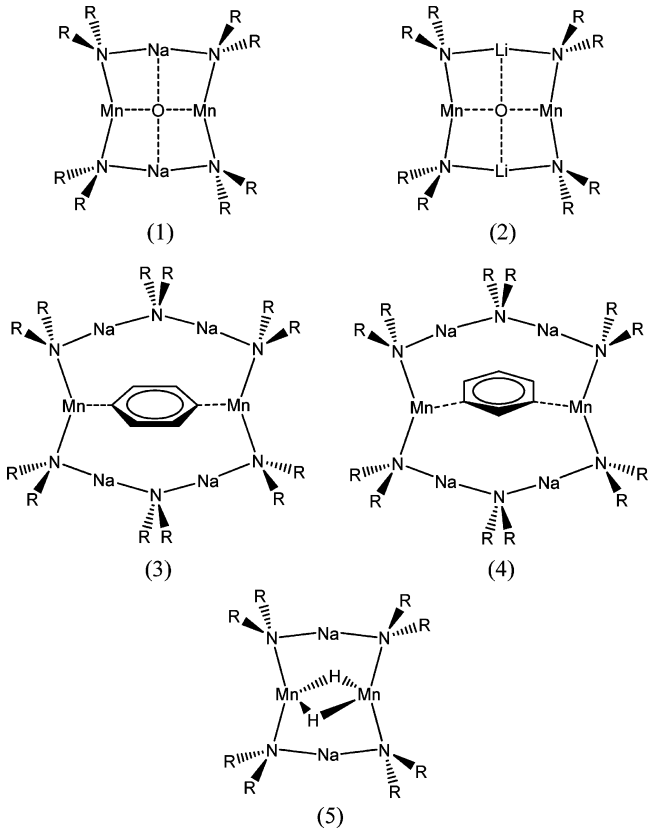

an appropriate mapping between computed electronic states and the states featured in the Heisenberg Hamiltonian.[13−16] The usefulness of BS-DFT to calculate magnetic interactions between Mn centers has been proven recently in different systems. Hence, model complexes of Mn(II) ions similar to those found in many biological systems have been recently studied theoretically using DFT methodologies, pointing out to the antiferromagnetic nature of the coupling between Mn(II) centers.[17] Further insight into the role of the bridging ligand in the magnetic coupling between Mn(IV) centers has been yielded by Rudberg et al.[18] Also, magnetic properties of mixed valence manganese (III, IV) dimers have been recently evaluated using broken-symmetry DFT methods.[19]

In the present paper a detailed theoretical study on the magnetic couplings based on the BS-DFT formalism between Mn(II) dimers forming part of five inverse crown structures is carried out. First, model systems of the five IC compounds where the substituents of the nitrogen atoms are replaced by hydrogen atoms will be validated by comparison to calculations of the "full" systems. Afterward, spin polarization maps and magnetic orbitals will be analyzed and discussed in order to rationalize the calculated J and discern the spin polarization pathways between Mn(II) centers. Finally, due to the dependence of the calculated J with the DFT exchange-correlation functional employed, a set of 10 functionals will be tested (5 pure and their corresponding hybridized versions) including the M05 developed by Zhao and Truhlar,[20] using two different basis sets of Pople type (6-31G(d,p) and 6-311++G(d,p)).

2. Computational Details

All the studied complexes are characterized by two magnetic metal centers with both sites exhibiting spins of $S = {}^5/_2$ for the two Mn(II) centers. Parallel and antiparallel coupling of the individual spins yields effective spins of $m_s = {}^{10}/_2$ for the high spin state (HS) and $m_s = 0$ for the broken-symmetry (BS) low spin state (LS). The Heisenberg−Dirac−van Vleck spin Hamiltonian is used to determine the energy ranking of spin states

$$\hat{H} = -2J\hat{S}_1\hat{S}_2 \tag{1}$$

where $\hat{S}_1$ and $\hat{S}_2$ are the respective spin angular momentum operators for atoms 1 and 2 and J is the effective exchange integral. A positive sign of J indicates a ferromagnetic interaction, whereas a negative sign indicates an antiferromagnetic interaction.

The broken symmetry formalism first proposed by Ginsberg[21] and Noodleman[16,22] and discussed and currently used by other authors[13,15,23−26] allows a reliable computation of the magnetic exchange coupling constant using a BS solution for the lowest spin-state.

Several equations have been proposed to calculate J depending on the overlap between magnetic orbitals or on the value of the averaged spin square momentum operator. In this work, the formula proposed by Yamaguchi et al.[13,27] where the dependence of J upon the overlap is replaced by a dependence upon the spin contamination of the broken symmetry solution will be employed

$$J = \frac{(E_{BS} - E_{HS})}{{}^{HS}\langle S^2\rangle - {}^{BS}\langle S^2\rangle} \tag{2}$$

where E_{BS} is the energy of the BS solution and E_{HS} is the energy of the HS state. For the BS-DFT calculations, the energy and wave function of the high-spin state is first computed, and then the orbitals are localized and used as an initial guess for the broken symmetry solution. Because of strong dependence of the magnetic coupling with respect to the exchange-correlation potential employed and the basis set, a set of ten approximated potentials will be used, namely, BLYP,[28,29] B3LYP,[30] OLYP,[31] O3LYP,[32] TPSS, TPSS0,[33] PBEPBE,[34,35] PBE0PBE,[36] M05, and M05−2X.[37] The ORCA package[38] has been used for all calculations except those carried out by the M05 and M05−2X potentials where Gaussian 03[39] was employed. Beacuse of the relevance of the basis set for the determination of accurate J values, the 6-31G(d,p) and 6-311++G(2d,2p) basis sets[40−43] were used for all atoms in order to evaluate the dependence of J with regard to the quality of the basis set. The program GAUSSVIEW was employed for the graphical representation of the spin polarization and molecular orbitals. It is worth noting that the studied complexes are highly unstable, decomposing in the presence of moisture or oxygen; therefore, the geometry determined experimentally by means of X-ray single crystal diffraction studies was employed for the calculations.

3. Results and Discussion

The inverse crown complexes considered in this study (**1**)−(**5**) present bulky ligands such as hmds in (**1**), tmp in (**2**)-(**4**), or N(iPr)$_2$ in (**5**) which makes their theoretical treatment difficult. Therefore, in order to carry out a complete study on the magnetic interactions between the Mn(II) centers using broken-symmetry DFT methodology, a more computationally tractable system is required. The proposed model system replaces the bulky amides (hdms, tmp, and N(iPr)$_2$) by lighter amides (NH$_2$) where the positions of the amide hydrogens are optimized at the B3LYP/

TABLE 1: Total Energies (au), Average $\langle S^2 \rangle$ Values, Total Spin on Mn Site, and Value of J (cm^{-1}) using Eq 2 for Complexes (1)−(5) in the Full and Model Systems Calculated at the B3LYP/6-31G(d,p) Level

B3LYP/6-31G(d,p)		state	E	$\langle S^2 \rangle$	spin Mn	spin O/C/H	J (cm^{-1})
FULL	(**1**)	HS	−6192.9984	30.02	4.75	0.21	−36.9
		LS-BS	−6193.0026	4.96	4.7	0	
	(**2**)	HS	−4024.5501	30.03	4.77	0.22	−41.6
		LS-BS	−4024.5548	4.97	4.73	0	
	(**3**)	HS	−5630.3187	30.03	4.75	0.03	−4.7
		LS-BS	−5630.3192	5.02	4.75	0.01	
	(**4**)	HS	−5669.5765	30.03	4.75	0.03	−3.2
		LS-BS	−5669.5768	5.02	4.75	0.01	
	(**5**)	HS	−3793.0396	30.02	4.82	0.00	−38.4
		LS-BS	−3793.0440	4.95	4.71	0.00	
MODEL	(**1**)	HS	−2925.2782	30.02	4.82	0.17	−30.3
		LS-BS	−2925.2816	4.97	4.77	0	
	(**2**)	HS	−2615.8579	30.02	4.85	0.2	−37.8
		LS-BS	−2615.8622	4.97	4.81	0	
	(**3**)	HS	−3517.2775	30.02	4.81	0.03	−1.5
		LS-BS	−3517.2776	5.02	4.81	0.01	
	(**4**)	HS	−3556.5473	30.02	4.81	0.04	−0.1
		LS-BS	−3556.5474	5.02	4.81	0.01	
	(**5**)	HS	−2851.2104	30.02	4.85	−0.01	−36.1
		LS-BS	−2851.2145	4.94	4.73	−0.01	

6-31G(d,p) level keeping frozen the remaining nuclei at their corresponding X-ray geometries. To test the validity of the model system, the HS and LS (using the broken-symmetry approach) states of complexes (**1**)−(**5**) considering both the full and the model ligands have been calculated at the B3LYP/6-31G(d,p) level method, which gives reasonable results.[44,45] The energetic results, $\langle S^2 \rangle$ eigenvalues, and Lowdin atomic spin densities are listed in Table 1.

Calculations at the B3LYP/6-31G(d,p) level for structures (**1**) and (**2**) bearing the full amide ligands yield medium antiferromagnetic couplings of −36.9 and −41.6 cm^{-1}, respectively, as expected for an oxygen bridge forming a 180° angle. Therefore, the Mn−Mn distance corresponds to twice the Mn−O distance. The fact that the binuclear units are well isolated and that the oxygen atom is the only magnetic exchange pathway is confirmed by very small variations upon substitution of the alkaline metal. In both cases, the obtained values are fairly similar although the effect of having a Li atom instead of a Na in the ICE structure produces an enlargement of the Mn−N distance from 2.091 (**1**) to 2.126 Å (**2**); the angle N−Mn−N is opened from 147.4° (**1**) to 169.7° (**2**), and a slight enlargement of the Mn−O distance from 1.927 (**1**) to 1.933 Å (**2**) is seen. Structures (**3**) and (**4**) present very weak antiferromagnetic couplings of −4.7 and −3.2 cm^{-1} as calculated at B3LYP/6-31G(d,p) level. The Mn−C distance increases from 2.201 (**3**) to 2.221 Å (**4**) and the Mn−N distance varies from 2.084 (**3**) to 2.092 Å (**4**), while the angle N−Mn−N changes slightly 145.7 (**3**) to 141.4° (**4**). The calculated results systematically overestimate the experimentally measured values of −0.7 and −0.1 cm^{-1}. The hydrido inverse crown (**5**) yields medium antiferromagnetic coupling of −38.4 cm^{-1} being the Mn−Mn distance of 2.827 Å and the Mn−H distance of 1.868 Å in good agreement with the measured value of −28.4 cm^{-1}.[10] Inspection of the atomic integrated spin polarization values show that for all the compounds nearly the ten unpaired electrons are located on the Mn nuclei (>4.80 e^- each). For compounds (**1**) and (**2**) there is also some spin polarization on the bridging oxygen in the high spin state (∼0.2 e^-) while for the LS state the net

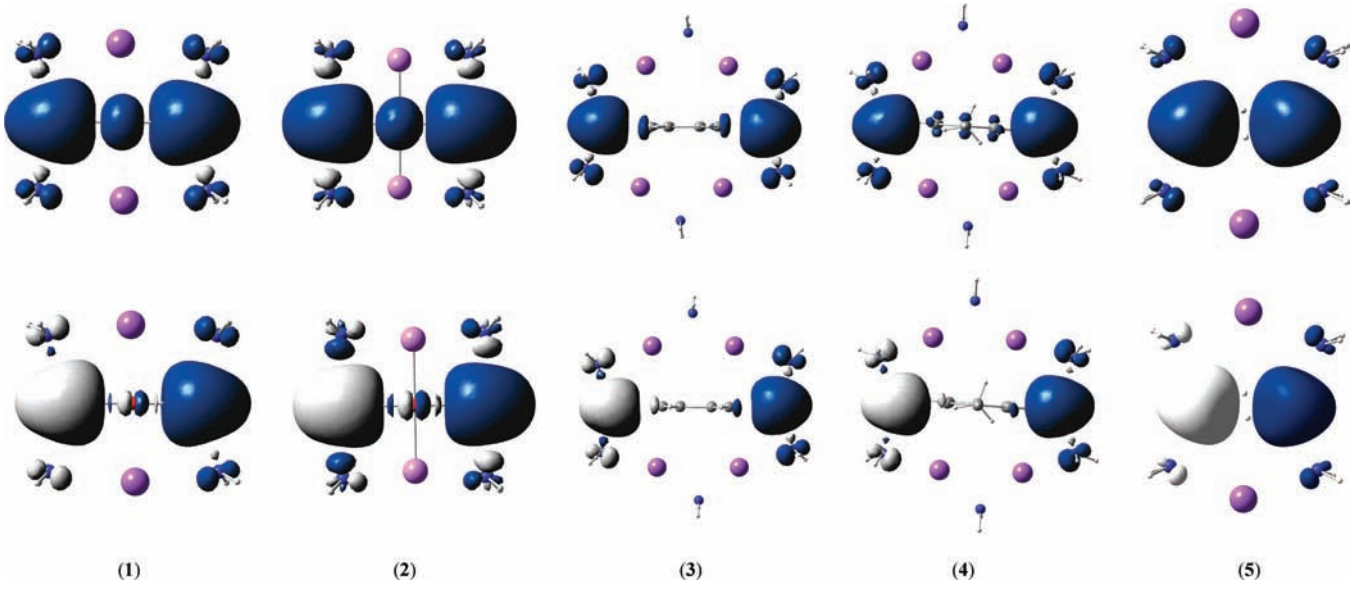

Figure 1. B3LYP/6-31G(d,p) spin polarization maps for the HS (up) and LS-BS (down) of model compounds (**1**)−(**5**). Blue/white for α/β spin density, respectively. Isocontour value = 0.003 (**1**)−(**4**) and 0.006 (**5**).

polarization is 0 due to the simultaneous spin polarization of different sign from both Mn centers. For compounds (**3**) and (**4**) carbon atoms of the bridging benzene present very small values of spin density, being the larger the carbon closer to the Mn centers. Finally, the hydrido bridge in compound (**5**) presents very small spin polarization values pointing out the absence of participation of the encapsulated hydride into the exchange mechanism. This can be confirmed by the relatively short distance between Mn centers (2.827 Å) which allows for a direct through space interaction while hydrogen atoms are lying outside the plane formed by the IC structure. For all compounds, the remaining spin density is distributed on the nitrogen atoms

Analysis of the calculated *J* values for the model systems of complexes (**1**)−(**5**) yield values in good agreement with those calculated for the full systems, although a systematic decrease of the antiferromagnetic interaction of 6.6 (**1**), 3.7 (**2**), 3.2 (**3**), 3.1 (**4**), and 2.3 cm^{-1} (**5**) can be appreciated. Inspection of the atomic spin polarization values for the full and model systems reveals that the replacement of secondary amide ligands by NH_2 produces a concomitant increase of the spin polarization of the Mn atoms and a decrease in the spin polarization of the bridging atoms. This result can be explained by the smaller spin polarizability of the NH_2 ligand in comparison to secondary amides. Therefore, it should be kept in mind that there is a small reduction (up to 6.6 cm^{-1} for (**1**)) of the *J* absolute values due to limitations on the model system. However, the present results fully justify the replacement of bulky ligands by hydrogen atoms for the calculation of magnetic interactions in ICE compounds considered in this work. Nevertheless, it should be remarked that the geometry of the ICE compounds is dependent on the nitrogen ligands and experimental synthesis of new ICE compounds would lead exchange coupling values far from those calculated for the model system.

Further insight into the exchange mechanism can be gained using spin polarization ($\eta(\alpha)-\eta(\beta)$) plots for compounds (**1**)−(**5**), (see Figure 1). These plots reveal that the unique exchange pathway connecting both Mn(II) nuclei takes place directly or through the anionic guest, discarding a possible pathway through the cationic ring. Hence, although the nitrogen atoms attached to the Mn centers are spin polarized, the presence of alkaline metals interrupts a possible exchange pathway across the cationic ring. Three types of exchange interactions can be observed depending on the nature of the guest ligand. In compounds (**1**) and (**2**), the bridging oxygen participates actively in the spin polarization pathway as it can be observed in Figure 1 and in agreement with the large values of *J*. In the HS state the oxygen atom presents a large and spherical spin polarization and of the same spin as Mn centers, while in the spin density for the BS solution that should be analyzed carefully because it is not a real state of the system, the oxygen is polarized toward the corresponding metallic center.

In compounds (**3**) and (**4**) the spin density on the atoms forming the benzene ring is very small (see Table 1). Although some amount of spin polarization at the carbon atoms attached to Mn centers can be observed, the π-system of the benzene ring it is not involved in the exchange mechanism yielding values of *J* close to 0. Finally, the spin polarization plot of compound (**5**) reveals that the exchange coupling is of direct type between Mn(II) centers without participation of the "guest" hydride as previously pointed out.[10]

The use of the magnetic orbitals allows a deeper understanding of the exchange pathways within the active electron approximation of the exchange interaction. The magnetic orbitals for the model compound (**1**) are plotted in Figure 2. The

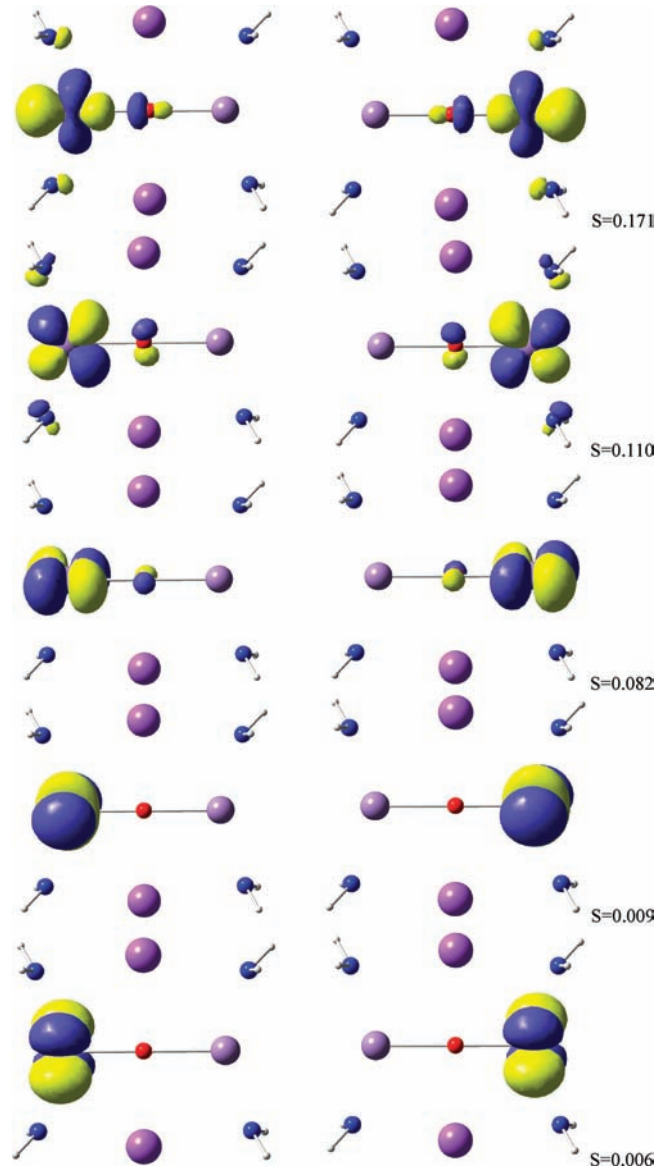

Figure 2. Isodensity surfaces (0.06) of the α (left) and β (right) spin magnetic orbitals and overlap (*S*) of the model inverse crown (**1**) at the B3LYP/6-31G(d,p) level obtained from the corresponding orbital transformation.

calculated overlap values between magnetic orbitals range from 0.171 ($d_{x^2-y^2}$), 0.110 (d_{xy}), 0.082 (d_{xz}), 0.009 (d_{z^2}), and 0.006 (d_{yz}). The three first sets of orbitals provide an antiferromagnetic pathway through the p atomic orbitals of oxygen. The larger overlap occurs between the $d_{x^2-y^2}$ orbital and the p_x orbital due to the sigma character of the interaction while the d_{xy} and d_{xz} orbitals interact with p_y and p_z orbitals of oxygen through a π-type interaction. The two last orbital sets of d_{z^2} and d_{yz} character participate only marginally in the exchange coupling. The overlaps for magnetic orbitals corresponding to the IC model compounds (**2**)−(**5**) are listed in the Supporting Information. Interestingly, the calculated *J* values increases with the magnitude of these overlaps.

The dependence of *J* for the model systems of inverse crowns (**1**)−(**5**) with respect to 10 different DFT approximate exchange correlation potentials and two basis sets (6-31G(d,p) and 6-311++G(2d,2p)) has been benchmarked (see Table 2). A strong dependence of the *J* value with the functional employed can be appreciated. Pure functionals overestimate systematically the magnitude of *J* compared to their hybridized versions as it

TABLE 2: Calculated Exchange Coupling Constants (J in cm^{-1}) for the Five Studied IC Compounds Using the Geometries of the Model System

	DFT method/basis set	BLYP	B3LYP	OLYP	O3LYP	PBEPBE	PBE0PBE	TPSS	TPSS0	M05	M05−2X	exptl
(**1**)	6-31G(d,p)	−61.1	−30.3	−47.2	−33.9	−52.8	−23.0	−46.9	−21.4	−36.8	−20.8	
	6-311++G(2d,2p)	−71.0	−35.3	−54.0	−39.2	−62.6	−27.3	−55.5	−25.1	−40.3	−22.6	
(**2**)	6-31G(d,p)	−75.3	−37.8	−59.4	−42.8	−65.9	−29.0	−59.5	−27.4	−43.7	−23.4	
	6-311++G(2d,2p)	−81.1	−40.2	−63.3	−45.2	−71.9	−30.8	−64.0	−28.9	−46.0	−23.8	
(**3**)	6-31G(d,p)	−3.5	−1.5	−2.9	−1.5	−3.2	−1.2	−2.6	−1.2	−1.3	−0.5	−0.7
	6-311++G(2d,2p)	−3.7	−1.4	−2.3	−1.5	−3.3	−1.4	−2.5	−1.3	−1.4	−0.4	
(**4**)	6-31G(d,p)	−1.4	−0.1	−0.6	−0.4	−1.2	0.4	−0.3	0.4	−0.4	−0.1	−0.1
	6-311++G(2d,2p)	−1.8	−0.2	−0.8	−0.4	−1.4	0.3	−0.8	0.5	−0.4	−0.1	
(**5**)	6-31G(d,p)	−82.7	−36.1	−57.9	−39.3	−65.5	−21.9	−56.6	−20.6	−49.8	−23.3	−28.4
	6-311++G(2d,2p)	−104.4	−46.1	−70.7	−48.5	−84.1	−29.1	−70.6	−26.2	−52.4	−24.0	

has been found in previous works[46,47] due to the inclusion of Hartree−Fock exchange. The performance of hybrid functionals is diverse; while B3LYP and O3LYP also overestimate severely the value of J, PBE0PBE, TPSS0, and M05−2X give similar values in good agreement with the experimental data available. Interestingly, the B3LYP/6-311++G(2d,2p) results overestimate the J values by nearly a factor of 2, which has been attributed to the effect of the self-interaction error of this exchange-correlation potential.[48] The effect of the basis set is almost negligible for weakly coupled complexes like (**3**) and (**4**), but it is significant for (**1**), (**2**), and (**5**), showing an increment in the magnitude of the antiferromagnetic coupling. This basis set dependence is much smaller for M05 and M05−2X functionals (up to 3.5 cm^{-1}) than for the others (up to 21.7 cm^{-1} for BLYP). Comparison with experimental data shows that the spin state ordering of complexes (**3**) and (**4**) is predicted correctly for all functional, except PBE0PBE and TPSS0 which yield ferromagnetic couplings for complex (**4**). On the other hand, PBE0PBE and TPSS0 combined with the 6-311++G(2d,2p) reproduce more accurately the experimentally measured J value for complex (**5**). The M05−2X functional, which according to previous theoretical studies[49,50] yields good results for exchange coupling calculations, predicts J values in reasonable agreement with experimental data.

4. Conclusions

This work presents a systematic investigation on the magnetic exchange interactions by means of broken-symmetry unrestricted DFT calculations in five novel inverse crown structures composed by binuclear Mn(II) compounds. Medium antiferromagnetic exchange couplings are predicted for those inverse crowns where the guest is an oxygen atom (**1**) and (**2**) or hydride (**5**), while very small antiferromagnetic exchange couplings are calculated for Mn dimers connected by a benzene ring deprotonated in either 1,4-(**3**) or 1,3-(**4**) positions. These calculated results are in very good agreement with experimental values available for complexes (**3**)−(**5**). The effect of the alkaline metal, the type of nitrogen ligands attached to the Mn atoms and the nature of the bridge have been analyzed, showing the strong influence of the bridging guest ligand and the very small effect of the structure of the cationic host in the value of J. Replacement of bulky amide ligands by NH_2, keeping frozen the geometrical parameters, produce a small reduction of J values. The mechanism of magnetic exchange coupling between the Mn(II) centers across a 180° bridged oxygen is revealed by means of the analysis of the magnetic orbitals. The dependence of the magnetic coupling with respect to the DFT exchange correlation functional and basis set has been assessed for the calculation of J in IC structures.

Acknowledgment. This work was supported by the Universitat Jaume I-Fundació Bancaixa, P1-1A2007-12. A.A. thanks support from the RyC program from the Ministerio de Educacion y Ciencia. The authors acknowledge the computer resources, technical expertise, and assistance provided by the Institute for Biocomputation and Physics of Complex Systems.

Supporting Information Available: Geometrical parameters (N−Mn−N angles and Mn−Mn distances), overlaps for the five magnetic orbitals for all model complexes calculated at B3LYP/6-31G(d,p) level and geometries (x,y,z coordinates in Å) of model (R = NH_2) inverse crown structures (**1**)−(**5**) are available in the Supporting Information. This information is available free of charge via the Internet at http://pubs.acs.org.

References and Notes

(1) Mulvey, R. E. *Organometallics* **2006**, *25*, 1060.
(2) Mulvey, R. E. *Acc. Chem. Res.* **2009**, *42*, 743.
(3) Forbes, G. C.; Kennedy, A. R.; Mulvey, R. E.; Rowlings, R. B.; Clegg, W.; Liddle, S. T.; Wilson, C. C. *Chem. Commun.* **2000**, *18*, 1759.
(4) Heathcock, C. H. *Comprehensive Carbanion Chemistry*; Buncel, E.; Durst, T., Eds.; Elsevier: New York, 1980.
(5) Carrella, L. M.; Clegg, W.; Graham, D. V.; Hogg, L. M.; Kennedy, A. R.; Klett, J.; Mulvey, R. E.; Renschler, E.; Russo, L. *Angew. Chem., Int. Ed.* **2007**, *46*, 4662.
(6) Kennedy, A. R.; Klett, J.; Mulvey, R. E.; Newton, S.; Wright, D. S. *Chem. Commun.* **2008**, *3*, 308.
(7) Blair, V. L.; Carrella, L. M.; Clegg, W.; Conway, B.; Harrington, R. W.; Hogg, L. M.; Klett, J.; Mulvey, R. E.; Rentschler, E.; Russo, L. *Angew. Chem., Int. Ed.* **2008**, *47*, 6208.
(8) Bomparola, R.; Davies, R. P.; Hornauer, S.; White, A. J. P. *Angew. Chem., Int. Ed.* **2008**, *47*, 5812.
(9) Albores, P.; Carrella, L. M.; Clegg, W.; Garcia-Alvarez, P.; Kennedy, A. R.; Klett, J.; Mulvey, R. E.; Rentschler, E.; Russo, L. *Angew. Chem., Int. Ed.* **2009**, *48*, 3317.
(10) Blair, V. L.; Carrella, L. M.; Clegg, W.; Klett, J.; Mulvey, R. E.; Rentschler, E.; Russo, L. *Chem.−Eur. J.* **2009**, *15*, 856.
(11) Negodaev, I.; de Graaf, C.; Caballol, R. *Chem. Phys. Lett.* **2008**, *458*, 290.
(12) Camacho, C.; Yamamoto, S.; Witek, H. A. *Phys. Chem. Chem. Phys.* **2008**, *10*, 5128.
(13) Soda, T.; Kitagawa, Y.; Onishi, T.; Takano, Y.; Shigeta, Y.; Nagao, H.; Yoshioka, Y.; Yamaguchi, K. *Chem. Phys. Lett.* **2000**, *319*, 223.
(14) Neese, F. *J. Phys. Chem. Sol.* **2004**, *65*, 781.
(15) Caballol, R.; Castell, O.; Illas, F.; Moreira, I. de P. R.; Malrieu, J. P. *J. Chem. Phys. A* **1997**, *101*, 7860.
(16) Noodleman, L. *J. Chem. Phys.* **1981**, *74*, 5737.
(17) Liu, S. B.; Perera, L.; Pedersen, L. G. *Mol. Phys.* **2008**, *105*, 2893.
(18) Rudberg, E.; Salek, P.; Rinkevicius, Z.; Agren, H. *J. Chem. Theor. Comp.* **2006**, *2*, 981.
(19) Orio, M.; Pantazis, D. A.; Petrenko, T.; Neese, F. *Inorg. Chem.* **2009**, *48*, 7251.
(20) Zhao, Y.; Truhlar, D. G. *Acc. Chem. Res.* **2008**, *41*, 157.
(21) Ginsberg, A. P. *J. Am. Chem. Soc.* **1980**, *102*, 111.
(22) Noodleman, L.; Case, D. A. *Adv. Inorg. Chem.* **1992**, 423.
(23) Bencini, A.; Totti, F.; Daul, C. A.; Doclo, K.; Fantucci, P.; Barone, V. *Inorg. Chem.* **1997**, *36*, 5022.
(24) Bencini, A.; Gatteschi, D.; Totti, F.; Sanz, D. N.; Mc Cleverty, J. A.; Ward, M. D. *J. Phys. Chem. A* **1998**, *102*, 10545.
(25) Ruiz, E.; Cano, J.; Alvarez, S.; Alemany, P. *J. Comput. Chem.* **1999**, *20*, 1391.
(26) Ciofini, I.; Daul, C. A. *Coord. Chem. Rev.* **2003**, *238*, 187.
(27) Yamaguchi, K.; Takahara, Y.; Fueno, T. *Applied Quantum Chemistry*; Smith, V. H., Eds.; Reidel: Dordrecht, 1986; pp 155.

(28) Becke, A. D. *Phys. Rev. A* **1988**, *38*, 3098.
(29) Lee, C. T.; Yang, W. T.; Parr, R. G. *Phys. Rev. B* **1988**, *37*, 785.
(30) Becke, A. D. *J. Chem. Phys.* **1993**, *98*, 1372.
(31) Handy, N. C.; Cohen, A. J. *Mol. Phys.* **2001**, *99*, 403.
(32) Cohen, A. J.; Handy, N. C. *Mol. Phys.* **2001**, *99*, 607.
(33) Tao, J. M.; Perdew, J. P.; Staroverov, V. N.; Scuseria, G. E. *Phys. Rev. Lett.* **2003**, *91*, 146401.
(34) Perdew, J. P.; Burke, K.; Ernzerhof, M. *Phys. Rev. Lett.* **1996**, *77*, 3865.
(35) Perdew, J. P.; Burke, K.; Ernzerhof, M. *Phys. Rev. Lett.* **1997**, *78*, 1396.
(36) Adamo, C.; Barone, V. *J. Chem. Phys.* **1999**, *110*, 6158.
(37) Zhao, Y.; Truhlar, D. G. *J. Chem. Theory Comp.* **2006**, *2*, 364.
(38) Neese, F. *ORCA an ab initio, density functional and semiempirical program package, Version 2.6.71*; Max-Planck institute for bioinorganic chemistry: Mulheim an der Ruhr, Germany, 2008.
(39) Frisch, M. J.; Trucks, G. W.; Schlegel, H. B.; Scuseria, G. E.; Robb, M. A.; Cheeseman, J. R.; Montgomery, J. A., Jr.; Vreven, T.; Kudin, K. N.; Burant, J. C.; Millam, J. M.; Iyengar, S. S.; Tomasi, J.; Barone, V.; Mennucci, B.; Cossi, M.; Scalmani, G.; Rega, N.; Petersson, G. A.; Nakatsuji, H.; Hada, M.; Ehara, M.; Toyota, K.; Fukuda, R.; Hasegawa, J.; Ishida, M.; Nakajima, T.; Honda, Y.; Kitao, O.; Nakai, H.; Klene, M.; Li, X.; Knox, J. E.; Hratchian, H. P.; Cross, J. B.; Bakken, V.; Adamo, C.; Jaramillo, J.; Gomperts, R.; Stratmann, R. E.; Yazyev, O.; Austin, A. J.; Cammi, R.; Pomelli, C.; Ochterski, J. W.; Ayala, P. Y.; Morokuma, K.; Voth, G. A.; Salvador, P.; Dannenberg, J. J.; Zakrzewski, V. G.; Dapprich, S.; Daniels, A. D.; Strain, M. C.; Farkas, O.; Malick, D. K.; Rabuck, A. D.; Raghavachari, K.; Foresman, J. B.; Ortiz, J. V.; Cui, Q.; Baboul, A. G.; Clifford, S.; Cioslowski, J.; Stefanov, B. B.; Liu, G.; Liashenko, A.; Piskorz, P.; Komaromi, I.; Martin, R. L.; Fox, D. J.; Keith, T.; Al-Laham, M. A.; Peng, C. Y.; Nanayakkara, A.; Challacombe, M.; Gill, P. M. W.; Johnson, B.; Chen, W.; Wong, M. W.; Gonzalez, C.; Pople, J. A. *Gaussian 03*, revision E.01; Gaussian, Inc.: Wallingford, CT, 2004.
(40) Hehre, W. J.; Ditchfield, R.; Pople, J. A. *J. Chem. Phys.* **1972**, *56*, 2257.
(41) Rassolov, V. A.; Pople, J. A.; Ratner, M.; Windus, T. L. *J. Chem. Phys.* **1998**, *109*, 1223.
(42) Krishnan, R.; Binkley, J. S.; Seeger, R.; Pople, J. A. *J. Chem. Phys.* **1980**, *72*, 65.
(43) Curtiss, L. A.; McGrath, M. P.; Blandeau, J. P.; Davis, V.; Binning, R. C.; Radom, L. *J. Chem. Phys.* **1995**, *103*, 6104.
(44) Ruiz, E. *Struct. Bond.* **2004**, *113*, 71.
(45) Comba, P.; Hausberg, S.; Martin, B. *J. Phys. Chem. A.* **2009**, *113*, 6751.
(46) Martin, R. L.; Illas, F. *Phys. Rev. Lett.* **1997**, *79*, 1539.
(47) Illas, F.; Martin, R. L. *J. Chem. Phys.* **1998**, *108*, 2519.
(48) Ruiz, E.; Alvarez, S.; Cano, J.; Polo, V. *J. Chem. Phys.* **2005**, *123*, 164110.
(49) Valero, R.; Costa, R.; Moreira, I. de P. R.; Truhlar, D. G.; Illas, F. *J. Chem. Phys.* **2008**, *128*, 114103.
(50) Ruiz, E. *Chem. Phys. Lett.* **2008**, *460*, 336.

JP907200U